

Screen-printed multicrystalline silicon solar cells with porous silicon antireflective layer formed by electrochemical etching

Jae-Hong Kwon

Display and Nanosystem Laboratory, College of Engineering, Korea University, Anam-dong, Seongbuk-gu, Seoul 136-701, Republic of Korea

Soo-Hong Lee

Strategic Energy Research Institute, Sejong University, 98 Kunja-Dong, Kwangjin-Gu, Seoul 143-747, Republic of Korea

Byeong-Kwon Ju^{a)}

Display and Nanosystem Laboratory, College of Engineering, Korea University, Anam-dong, Seongbuk-gu, Seoul 136-701, Republic of Korea

(Received 10 January 2007; accepted 25 March 2007; published online 31 May 2007)

The latest results on the use of porous silicon (PS) as an antireflection coating (ARC) in simplified processing for multicrystalline silicon (mc-Si) solar cells are presented. A PS layer with optimal antireflection characteristics was obtained for charge density (Q) of 5.2 C/cm^2 . The weighted reflectance was reduced to 4.7% in the range of wavelengths between 400 and 1000 nm. Also, the optimization of a PS selective emitter formation results in a 13.2% efficiency mc-Si cell ($2 \times 2 \text{ cm}^2$) with the electroplating method. Specific attention is given to the implementation of a PS ARC into a commercially compatible screen-printed solar cell process. © 2007 American Institute of Physics. [DOI: 10.1063/1.2735413]

I. INTRODUCTION

Light trapping is an important method of increasing the efficiency of crystalline silicon solar cells. Several other techniques such as the surface antireflection layer (ARC) (Ref. 1) and texturization² have been used widely for the same purpose. Commercial multicrystalline silicon (mc-Si) solar cells have, in general, silicon-nitride (SiN_x) films that not only act as an ARC with a suitable refractive index, but also improve the performance of photovoltaic devices by defect, surface, and bulk passivation. However, the formation of the SiN_x films by using plasma enhanced chemical vapor deposition (PECVD) (Ref. 3) is a costly process. On the other hand, recently, simple and low-cost techniques that use chemical solutions have been developed to solve the cost problem. For example, alkaline etchants composing NaOH or KOH with isopropyl alcohol (IPA) as an organic agent are widely used to texture monocrystalline silicon (mono-Si).⁴ However, this method is not efficient for mc-Si because only a certain fraction of the grains have the (100) crystallographic orientation. Acidic etching by HF and HNO_3 , which act as strong oxidizing agents, has been used to texture the surface of mc-Si.⁵ However, with this technique, it is also difficult to control the uniformity of the Si wafer surface and layer thickness, and other approaches have been also studied.^{6,7}

Porous silicon (PS) ARC has several advantages such as production of lower reflectance than that of the deposited

single ARC, no vacuum processes or toxic gasses, PS formation in $<35 \text{ s}$ with good repeatability, simplicity, and low cost.

Different authors have proposed to use PS as a single layer or multilayer ARC,^{8,9} light diffuser,¹⁰ backside reflector,¹¹ and blue-to-red light transformer.¹² A significant improvement of optical confinement was found after PS formation.

ARC can be optimized by tailoring the porosity (or refractive index) of the PS layer for a given cell structure. Through this optimization, surface geometry can be optimized. Since PS texturing does not depend on crystallographic orientation, mc-Si can be uniformly textured on the whole wafer when the mc-Si surface is supplied by high current density. However, the mc-Si solar cells using PS ARC have low efficiency due to a contact degradation due to the interaction of HF acid and silver (Ag), namely, etching of the glass frit in the Ag paste by the HF acid contained in the etching solution by increasing the contact resistivity.¹³ Therefore, screen-printed front contact should be protected.

In this paper, we present several promising results: our technique provides weighted reflectance that is 4.7% in the wavelength range of 400–1000 nm lower than those of other techniques. Also, to avoid such degradation of screen-printed front contact, pure Ag was electroplated on the front contact using a light-induced plating method.

II. EXPERIMENT

A. The device fabrication

A p -type mc-Si Eurosolar wafer with a thickness of $330 \mu\text{m}$ and a resistivity of $0.5\text{--}2 \Omega \text{ cm}$ was used to fabricate the screen-printed solar cell. At first, saw damage from

^{a)} Author to whom correspondence should be addressed; electronic mail: bkju@korea.ac.kr; FAX: +82-2-920-1325; homepage: <http://diana.korea.ac.kr>

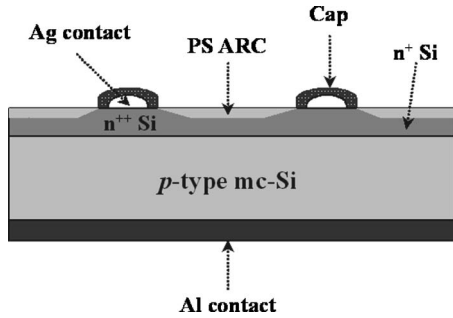


FIG. 1. The cross-sectional diagram of the mc-Si solar cell structure using the PS ARC with Ag cap.

the wire-sawing process was removed using an alkaline solution. During saw damage removal, the surface of the Si wafer was slightly textured, and a small decrease in the surface reactance occurred.⁶ Before the emitter diffusion process, the wafer was cleaned in baths of RCA I, RCA II, and HF solutions to remove organic materials, metal impurities, and the silicon-oxide layer at the surface of the Si wafer, respectively. The *n*-type emitter was formed by heavily doping with phosphorus using a POCl_3 source at high temperature. The sheet resistance of the surface was set to $30 \Omega/\text{sq}$ after etching of the phosphorous silicate glass (PSG). Then, Ag and Al pastes were screen printed on the front and the rear sides of the wafer to form metal electrodes. Two firing processes, Al firing at the rear side, and an Ag firing through process, were carried out at one time in this cell fabrication scheme. Next, front contact was electroplated by Ag using a light-induced plating method to avoid degradation of screen-printed front contact. Finally, PS film was formed on the front surface of the cell by electrochemical etching (ECE). Thus, this process provides self-aligned selective emitter etching to be used at the same time as an efficient ARC. The general view of the final cell structure is presented in Fig. 1.

B. Porous silicon formation

The ECE was performed by using a mixed solution containing (i.e., 3:1 volume ratio mixture of 49% HF solution and absolute $\text{C}_2\text{H}_5\text{OH}$). PS formation by ECE with multi-channel Potentiostat/Galvanostat. ECE current density ($10\text{--}270 \text{ mA}/\text{cm}^2$) and duration ($1\text{--}35 \text{ s}$) were controlled by computer-driven potential-stabilized electrolyte bath. The bath contained polytetrafluoroethylene (PTFE), and the platinum (Pt) electrode was used as a cathode. Counter electrode was used as Si wafer/Pt. The bath was agitated by a magnetic stirring bar to prevent H_2 bubbling over the etching surface and thus, fabricate a more uniform PS structure. After PS formation, samples were rinsed with DI water and were dried immediately after ECE to prevent the PS film from flaking and deterioration (i.e., the sample was dried in N_2 gas and stored).

C. Measurements

The weighted reflectance measurements were carried out by using the reflectance tool in the $300\text{--}1000 \text{ nm}$ wavelength range. The surface morphology of the PS formed by the ECE was observed by field emission scanning electron micro-

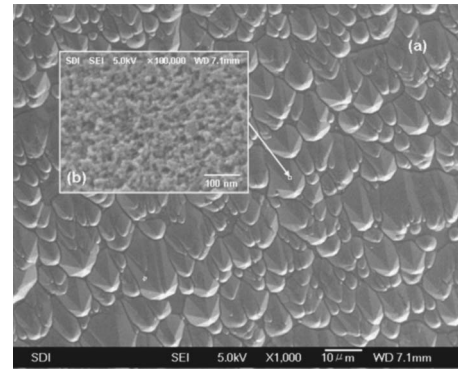


FIG. 2. The FE-SEM image taken from the surface of the PS samples prepared using $Q=5.2 \text{ C}/\text{cm}^2$ in HF: $\text{C}_2\text{H}_5\text{OH}$ electrolyte with a volumetric ratio of 3:1. (a) The PS formation after alkaline-textured mc-Si ($\times 1000$), (b) the mezoporous structure ($\times 100\,000$).

scope (FE-SEM). The ECE of Si, from which we obtained the thickness and porosity of the PS layer, was analyzed by spectroscopic ellipsometer (SE). Also, the cell characteristics were measured under the AM 1.5 spectrum ($100 \text{ mW}/\text{cm}^2$) at 25°C with the SPI-CELL TEST 150 system.

III. RESULT AND DISCUSSION

Several PS samples were investigated as a function of the current density (J) and total etching time, while the total charge density (Q) injected per unit area (with the total amount of Si removed) was kept constant during etching.¹⁴ The high current density ($270 \text{ mA}/\text{cm}^2$) and short anodic ECE time ($<35 \text{ s}$) formed a high-porosity-like mezoporous structure. PS surface images in Fig. 2 show that the formation of PS is isotropic and has little dependence on Si surface crystallographic orientation because of a rapidly formed uniform PS film.¹⁵ Figure 2(b) shows the top view of a PS layer. The surface geometry was a new surface structure composed of a standard texture formed by KOH etching and mezoporous substructure with a pore diameter smaller than 50 nm in Fig. 2(b). We observed an interesting mezoporous spongelike structure suitable for light trapping and light diffusing as an ARC since the charge density increases, the porosity increases, and the index of refraction decreases. In particular, we have previously studied correlation between the reflectance and the surface roughness.¹⁶ The reduction of reflectance could be explained by the higher roughness of the surface after PS formation.

The optical reflectivity of this structure decreased dramatically about 4.7%, as presented in Fig. 3. Analyzed by SE,¹⁷ the thickness and porosity of the PS layer obtained by ECE of Si were $400\text{--}500 \text{ \AA}$ and $80\%\text{--}90\%$, respectively. Visually a top PS layer exhibited still homogeneous blue color and can be sufficiently used as an ARC for solar cells.

Figure 3 shows the weighted reflectance as a function of wavelength for three samples with $Q=1.3$, 3.2 , and $5.2 \text{ C}/\text{cm}^2$ (listed in Table I). The reflectance decreased to less than 5% for $Q=5.2 \text{ C}/\text{cm}^2$, between 400 and 1000 nm . The reflectance spectra in Figs. 3(a)–3(c) provide the optical properties for PS film. The specific form of the reflectance spectra of the grains covered with a PS layer is due to interference effects in the layer, which implies that the PS layer

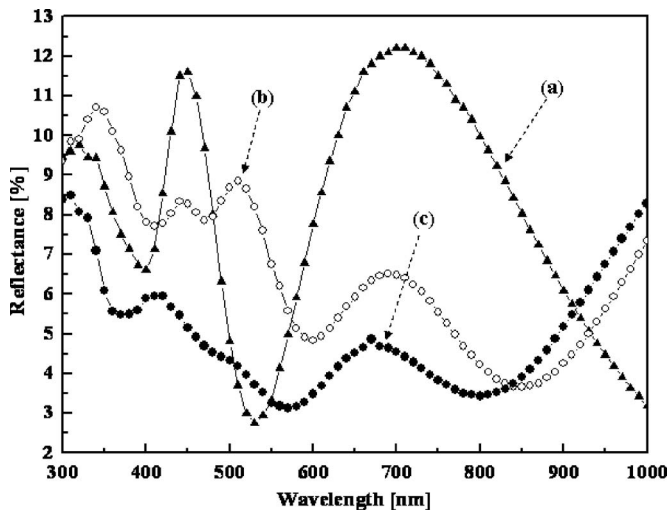


FIG. 3. Plots of the measured reflectance spectra of PS films grown at 1.3, 3.2, and 5.2 C/cm² in the wavelength range of 300–1000 nm. These films show weighted reflectance as (a) 8.0%, (b) 6.0%, and (c) 4.7% in the wavelength range of 400–1000 nm.

has different optical properties compared to bulk Si.¹⁸ Figures 3(a)–3(c) show the relationship between increases in porosity and decreases in reflective index for PS films. The number of modulations in the spectra directly corresponded to the number of various refractive indexes in the PS layer. Further increase of Q did not significantly change the reflectance. When using high charge densities (>8.1 C/cm²), the modulations may not be observed at all because the PS layer obtained by ECE is peeled off. We observed flaked and deteriorated PS film generated at 9.5 C/cm².

The integral reflectance of PS in Fig. 3(c) is 4.44 in the wavelength range of 650–700 nm. The decrease in the reflectance in the sensitivity range of the solar cell increases the short circuit current density (J_{sc}) (Fig. 5 and Table II). The wavelength range is important for photovoltaic applications since the energy content of the solar spectrum peaks in that range. Minimum reflectance occurred at charge density 5.2 C/cm². In addition, the PS structure generally is assumed to give rise to quantum confinement and an increased band gap. The wide band gap of PS might be useful to establish a minority carrier mirror, which could contribute to surface passivation.

Figure 4 shows that the additional PS ARC after the alkaline-textured mc-Si wafer results in a decrease in reflectance. It is clearly observed that the reflectance of the PS ARC used in further experiments has a minimum of 3.1% at 570 nm, while the SiN_x ARC reflectance has a minimum of 2.0% at 730 nm. As a result, the weighted reflectance of the PS used as an ARC is 4.7% in the wavelength range from 400 to 1000 nm and 8% less than that of a commercial SiN_x

TABLE I. Weighted reflectance (R) from three different PS formation conditions of charge density (Q).

	(a)	(b)	(c)
Q (C/cm ²)	1.3	3.2	5.2
R (%)	8.0	6.0	4.7

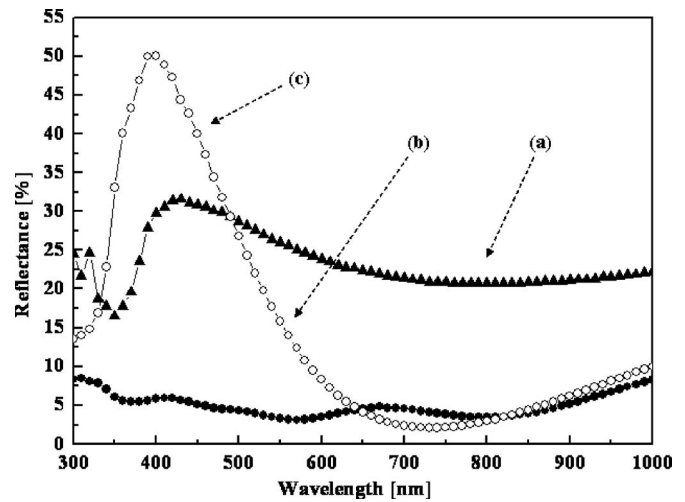


FIG. 4. Reflectance characteristics of (a) alkaline-textured mc-Si wafer, (b) PS ARC, and (c) single-layer SiN_x ARC.

ARC. Moreover, we compared the reflectance characteristics of the optimized SiN_x layer coated (thickness of 700–800 nm) by PECVD with a PS layer.

A comparison of optimal PS ARC formed on alkaline-textured mc-Si surface and conventional SiN_x ARC formed on alkaline-textured mc-Si surface shows some advantages. First, PS ARC is formed uniformly on the whole area of the mc-Si wafer almost independently of the grain orientation, while conventional alkaline texturing only works well in the case of mono-Si. Second, The PS ARC demonstrated optical performance superior to most vacuum-deposited SiN_x ARC layers, as shown in Fig. 4. It is expected that the perfect light diffuser for broad wavelength could be used as an ARC without other materials of ARC. Moreover PS has some passivating capabilities, which allow fabricating solar cells without an additional passivation coating.

The method of ECE considerably exceeds traditional methods of chemical anisotropic and mechanical texturing in the efficiency of optical losses reduction by decreasing weighted reflectance in the range from 400 to 1000 nm to 4.7%. Besides, the ECE method allows forming texture on

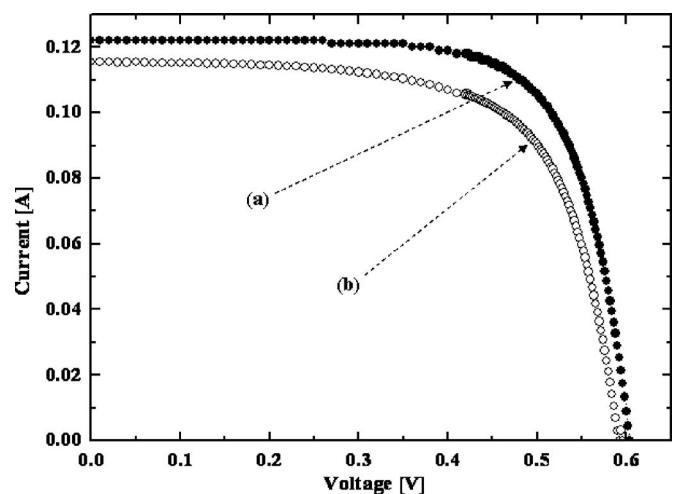


FIG. 5. Illuminated current-voltage characteristics of the mc-Si solar cell using the PS ARC at (a) 4.0 C/cm² and (b) 1.6 C/cm².

TABLE II. *I*-*V* characteristics of mc-solar cell after PS ARC formation at (a) 4.0 C/cm² and (b) 1.6 C/cm².

	(a)	(b)
Charge density	4.0 C/cm ²	1.6 C/cm ²
V_{oc}	604 mV	585 mV
J_{sc}	30.5 mA/cm ²	28.9 mA/cm ²
Fill factor	0.721	0.676
Efficiency	13.27 %	11.43 %

the surface of already created solar cells both before deposition of frontal contact comb and after its formation without additional photolithography process. Because of that, the technological process of solar cell structure creation is simplified.

Figure 5 and Table II show the performance parameters of solar cells illuminated *I*-*V* characteristics of the mc-Si solar cells using PS ARC (mezoporous structure) at (a) 4.0 C/cm² and (b) 1.6 C/cm². The charge density enhancement may be ascribed to both the antireflection properties of PS and a better blue color of the selective emitter. The boost in open circuit voltage (V_{oc}) is related to the increase in short circuit current (I_{sc}) and probably also to a lower recombination velocity at the Si/PS interface since it has been demonstrated that PS has some passivating capabilities arising from the presence of Si hydrides and Si hydroxides.¹⁹

IV. CONCLUSION

The study carried out in this paper demonstrated that by the PS ARC technique optimization it is possible to create new morphology of the Si surface structure. This layer acts as a perfect light diffuser and provides an appropriate reflectance which is quite comparable to the reflectance of an alkaline-textured Si surface covered by the conventional SiN_x ARC layer. This approach showed the performance parameters including 13.27 efficiency of the cell. V_{oc} of the cell is 604 mV and I_{sc} is 122 mA. Simplicity and low cost of the

ECE technique as well as its adaptation to the silicon solar cell manufacturing provide for a very promising technology in an industrial process.

ACKNOWLEDGMENTS

The authors thank Dae-Woon Kim (Energy Laboratory Corporate R&D Center, Samsung SDI Co. Ltd., Suwon, Republic of Korea) for help during this work. The authors are indebted to Dong-Seop Kim (Georgia Institute of Technology, Atlanta, GA) for discussion.

- ¹J. Zhao, A. Wang, P. Altermatt, and M. A. Green, *Appl. Phys. Lett.* **66**, 3636 (1995).
- ²H. Saha, S. K. Datta, K. Mukhopadhyay, S. Banerjee, and M. K. Mukherjee, *IEEE Trans. Electron Devices* **39**, 1100 (1992).
- ³L. Asinovsky, F. Shen, and T. Yamaguchi, *Thin Solid Films* **313-314**, 198 (1998).
- ⁴P. Campbell and M. A. Green, *J. Appl. Phys.* **62**, 243 (1987).
- ⁵R. W. Fathauer, T. George, A. Ksendzov, and R. P. Vasquez, *Appl. Phys. Lett.* **60**, 995 (1992).
- ⁶S. W. Park, J. Kim, and S. H. Lee, *J. Korean Phys. Soc.* **43**, 423 (2003).
- ⁷H. G. Craighead, R. E. Howard, and D. M. Tennant, *Appl. Phys. Lett.* **37**, 653 (1980).
- ⁸M. Lipiński, S. Bastide, P. Panek, and C. Lévy-Clément, *Phys. Status Solidi A* **197**, 512 (2003).
- ⁹M. Lipinski, P. Panek, E. Beltowska, and H. Czernastek, *Mater. Sci. Eng. B* **101**, 297 (2003).
- ¹⁰R. Bilyalov, C. S. Solanki, J. Poortmans, O. Richard, H. Bender, M. Kummer, and H. Von Känel, *Thin Solid Films* **403-404**, 170, 2002.
- ¹¹J. Zettner, M. Thoenissen, T. Hierl, R. Brendel, and M. Schulz, *Prog. Photovolt. Res. Appl.* **6**, 423 (1998).
- ¹²O. Nichiporuk, A. Kaminski, M. Lemiti, A. Fave, S. Litvinenko, and V. Skryshevsky, *Thin Solid Films* **511-512**, 248 (2006).
- ¹³K. Firor and S. Hogan, *Sol. Cells* **87**, 5 (1981).
- ¹⁴E. V. Astrova, T. N. Borovinskaya, A. V. Tkachenko, S. Balakrishnan, T. S. Perova, A. Rafferty, and Y. K. Gun'ko, *J. Micromech. Microeng.* **14**, 1022 (2004).
- ¹⁵M. Ben Damiani, Ph.D. thesis, Georgia Institute of Technology, 2004.
- ¹⁶R. J. Martín-Palma, L. Vázquez, J. M. Martínez-Duart, M. Schnell, and S. Schaefer, *Semicond. Sci. Technol.* **16**, 657 (2001).
- ¹⁷S. Strehlke, D. Sarti, A. Krotkus, O. Polgar, M. Fried, and C. Lévy-Clément, in *Photochemistry, PV 97-20*, edited by A. Fujishima *et al.*, The Electrochemical Society Proceedings Series (The Electrochemical Society, Pennington, NJ, 1997), p. 278.
- ¹⁸R. Bilyalov, C. S. Solanki, J. Poortmans, O. Richard, H. Bender, M. Kummer, and H. von Känel, *Thin Solid Films* **403-404**, 170 (2002).
- ¹⁹R. R. Bilyalov, R. Ludemann, and S. Schaefer, *Sol. Energy Mater. Sol. Cells* **60**, 391 (2000).